

1     **A laboratory desert dust generator using vibration on a**  
2     **soil sample: mineralogical and compositional study**

3     **Z. Qu<sup>1,2</sup>, A. Trabelsi<sup>3</sup>, R. Losno<sup>1</sup>, F. Monna<sup>4</sup>, S. Nowak<sup>5</sup>, M. Masmoudi<sup>3</sup>, and**  
4     **J.P. Quisefit<sup>2</sup>**

5             <sup>1</sup>Université de Paris, Institut de Physique du Globe de Paris, UMR CNRS 7154, France

6             <sup>2</sup>LISA – Université Paris Est Créteil, Université de Paris, UMR CNRS 7583, Créteil, France

7             <sup>3</sup>Faculté des Sciences de Sfax, Sfax University, Tunisia

8             <sup>4</sup>ArtéHis - UMR CNRS 6298, Université de Bourgogne-Franche Comté, Dijon, France

9             <sup>5</sup>Université de Paris, RX Facility, Department of Chemistry, France

10     **Key Points:**

- 11     • aerosol generation  
12     • compositional analyses

---

Corresponding author: Remi Losno, losno@ipgp.fr

## Abstract

A laboratory study was carried out using a vibrating system (SyGAVib) to produce particles from four soils collected in the central Tunisian region around Sfax. The aim of this device is to mimic dust emission by natural wind erosion. Using compositional analysis, the dust produced was compared to: (i) dust generated in a wind tunnel by the same soils, (ii) fine sieved and (iii) original bulk soils, and (iv) naturally occurring aerosol samples collected in the same area. The relative quartz content strongly decreases from bulk to fine soils, and again from fine soils to both wind tunnel and vibration generated aerosols. Compositional data analysis (CoDA) clearly shows: (i) a silica dilution effect in bulk soils, and (ii) that if silica is removed from the composition, the elemental compositions of fine soils and generated aerosols are similar but differ from bulk soils. Both aerosol generation methods produce material with chemical compositions that are also close to those measured in field-sampled aerosols, and the fine soil composition is much closer to that of field and laboratory aerosols than to the parent soil. Aerosols generated from soils in the laboratory, either using a vibrating system or a wind tunnel, can be used as surrogates of the particles collected directly in the field.

## Plain Language Summary

A laboratory study was carried out using a vibrating system (SyGAVib) to produce particles from four soils collected in the central Tunisian region around Sfax. The aim of this device is to mimic dust emission by natural wind erosion. The chemical composition of the dust produced was compared to another dust generator (a wind tunnel), fine sieved soil, original bulk soils, and finally naturally occurring dust found in the same area. Both dust generators produce similar samples which look very different from bulk soils.

## 1 Introduction

Mineral dust is extensively studied because its emission due to wind erosion in arid and semi-arid regions of the Globe accounts for approximately 30 to 50% of the total aerosol injections in the troposphere (Andreae, 1995). Mineral dust emission by wind erosion can be driven by direct aerodynamic resuspension (Kjelgaard et al., 2004), saltation bombardment and aggregate disintegration (Gomes et al., 1990). Only the finest particles can remain in suspension in the atmosphere and be transported over thousands of kilometres from their emission areas (Arimoto, 2001). Consequently, the chemical composition of transported soil-derived dust is related to the fine fraction of soil particles and the use of the bulk source soil chemical composition as a surrogate for the dust chemical composition may result in systematic biases.

Natural dust emission from a given source is strongly dependent on local meteorological conditions and is difficult or even impossible to isolate from advection coming from elsewhere. Artificial dust production in the field or laboratory is an alternative way to study the source of the soil dust. Gillette (1978) investigated dust emission by wind erosion using a straight-line wind tunnel laid on the ground and Alfaro & Gomes (1995) brought soil into a wind tunnel mounted in their laboratory. Although the wind tunnel directly simulates the natural wind erosion process under controlled wind conditions, it is difficult to use due to the large amount of soil that needs to be brought back to the laboratory. To work at a laboratory bench scale, Lafon et al. (2014) generated desert dust by shaking soil samples in an Erlenmeyer flask, Engelbrecht et al. (2016) blown fine soil in a closed cabinet, Salam et al. (2006) generated aerosol by vibrating soil samples using a loudspeaker to study the ice nucleation efficiency and Mendez et al. (2013) used a rotating drum. For further details regarding previous experiments see the extensive review on aerosol generation published by Gill et al. (2006). Note that some authors simply used fine sieved soils as dust analogues (Guieu et al., 2014).

**Table 1.** Soil characteristics using the WRB classification derived from dry sieving with a stainless steel system. El Attaya and El Hsar are located on Kerkennah Island. The finest fraction contains aggregated silt and clay particles.

Soil name	El Attaya	El Hsar	Cherarda	Ghraïba
Location (WG84)	34°44'N 11°18'E	34°42'N 11°09'E	35°22'N 10°10'E	34°24'N 10°18'E
Nature	oolitic limestone	continental silt	limestone bed	alluvium and wind sand
Soil Fraction				
Coarse and medium sand ( $> 200 \mu\text{m}$ )	30.0%	44.2%	35.9%	69.1%
Fine and ultra-fine sand (between $63$ and $200 \mu\text{m}$ )	61.5%	48.2%	59.9%	29.0%
Silt and clays ( $< 63 \mu\text{m}$ )	8.5%	7.6%	4.2%	1.9%

63 Here, a new soil-derived dust generator has been developed. It is based on controlled  
 64 vibration waves and requires a very small amount of bulk soil. The aim of this paper is  
 65 to chemically compare the material produced by this new device with aerosols generated  
 66 by the wind tunnel, fine mesh sieved soil and original bulk soil. Chemical changes are  
 67 evaluated using compositional analyses, a set of statistical tools especially designed for  
 68 handling chemical compositions in a clear and concise manner (Pasquet et al., 2016; Monna  
 69 et al., 2017).

## 70 2 Experimental, Materials and Methods

### 71 2.1 soil sampling

72 In order to generate aerosols in the laboratory, four different surface bulk soil sam-  
 73 ples of approximately 10 kg each were collected in the Sfax region, Tunisia (see Table 1  
 74 for the sampling locations and physical properties). They were first coarse sieved (2 mm).  
 75 Approximately 100 g of all collected soils were dry sieved with a stainless steel system  
 76 to determine their texture (Table 1, supporting information Table S1). A fraction smaller  
 77 than  $56 \mu\text{m}$  was also sieved on a nylon mesh for further comparison with generated aerosols.

### 78 2.2 Aerosol generation

79 Approximately 0.3 g of soil was placed into an open-top  $\approx 20$  mL polyethylene cup  
 80 that was fixed on top of a loudspeaker (Figure 1). Vibrations from the loudspeaker (sine-  
 81 wave frequency = 100 Hz) levitated the soil particles, while collisions broke up the largest  
 82 aggregates, favouring the emission of fine particles. The dust generation cup was placed  
 83 at the bottom centre of an upright stainless steel cylinder measuring 125 mm in diam-  
 84 eter. Two air inlets were positioned at the bottom of the tube; a third air inlet directed  
 85 toward the top centre of the soil container created a local turbulence, which improved  
 86 the extraction of the particles. An external pump and an optical particle counter, with  
 87 flow rates of  $5.5 \text{ L min}^{-1}$  and  $2.8 \text{ L min}^{-1}$  respectively, were connected to the top of the  
 88 cylinder to maintain a constant upwards air flow within the system. The total ascend-  
 89 ing flow rate was approximately  $8 \text{ L min}^{-1}$ , providing a vertical air velocity of  $\approx 1.1 \text{ cm s}^{-1}$ .  
 90 According to Stoke's steady state equations, and assuming spherical particles with a den-  
 91 sity of  $2.2 \text{ g cm}^{-3}$ , only particles smaller than  $\approx 10 \mu\text{m}$  were carried up to the top of the  
 92 cylinder. Particles were collected during 40 min on a polycarbonate membrane filter (32 mm

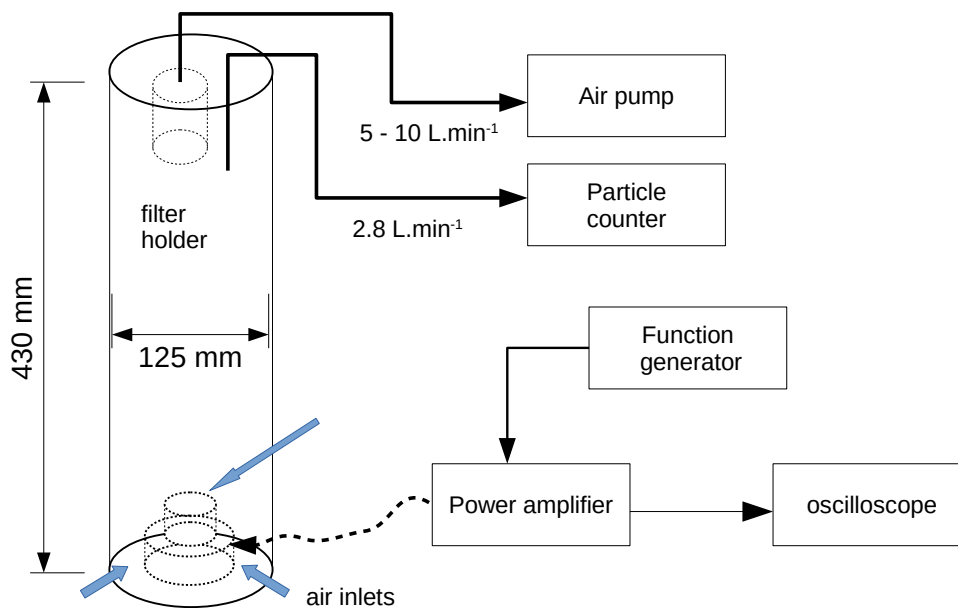


**Figure 1.** Diagram of the SyGAVib system

93 in diameter, and with a pore size of 0.4  $\mu\text{m}$ ). The whole system was placed in a verti-  
 94 cal laminar flow hood to prevent any external contamination.

95 The laboratory wind tunnel generator is extensively described in Alfaro & Gomes  
 96 (1995) and Alfaro et al. (1997). In practice, approximately two kilograms of soil were  
 97 placed at the bottom of the wind tunnel (30x30x400 cm<sup>3</sup>), and an air flow of approx-  
 98 imately 5 m s<sup>-1</sup> was applied to generate aerosols for several minutes (2 to 15 depend-  
 99 ing on the generated dust concentration), This simulated wind speed induces a friction  
 100 velocity large enough to produce saltation and simulates wind erosion with a process oc-  
 101 ccurring under natural conditions. The generated aerosol was pumped at mid-height (10 cm)  
 102 through a 30  $\mu\text{m}$  cut-off diameter decanter, as described in Alfaro (2008), and deposited  
 103 on similar polycarbonate filter membrane as that used for the SyGAVib experiments.

104 For each soil origin, aerosol generation was replicated 5–6 times by the wind tun-  
 105 nel device and 3–5 times by the SyGAVib device. At least one replicate was loaded to  
 106 the maximum dust amount for mineralogical determinations by X-Ray diffraction (XRD),  
 107 while the other filters were adequately loaded for further elemental analysis using X-Ray  
 108 fluorescence spectrometry (XRF).

### 109 2.3 Soil and aerosol analyses

110 Chemical analyses were performed on the bulk soil and fine soil (BS and FS respec-  
 111 tively) using energy dispersive X-ray Fluorescence spectrometry (EDXRF, Epsilon, PAN-  
 112 alytical). Aerosol filters obtained with the wind tunnel (WT) and the SyGAVib (Syg)  
 113 system were analysed directly on the membrane filter in thin layer conditions for aerosols  
 114 (Losno et al., 1987). Soil samples were first finely ground in a tungsten carbide ball mill  
 115 and 5 g of the fine powder was transformed into a pressed pellet with an addition of 0.9 g  
 116 of wax for the EDXRF analyses. Soil pellets were then analysed as infinite thickness lay-  
 117 ers using the Ominan® software, which deconvolves spectra from the background and  
 118 from the line overlaps, and empirically corrects matrix effects. A detection limit of a few  
 119  $\mu\text{g g}^{-1}$  is obtained for most elements. The initial calibration was established using 13 cer-

120 tified reference materials from SARM (Nancy): Anorthosite AN-G, Basalt BE-N, Basalt  
121 BR, Bauxite BX-N, Diorite DR-N, Disthene (Kyanite) DT-N, Granite AC-E, Gran-  
122 ite GA, Granite GS-N, Granite MA-N, Phlogopite Mica-Mg, Potash Feldspar FK-N,  
123 and Serpentine UB-N.

124 Structural analyses were performed by XRD using an EMPYREAN (PANalytical)  
125 diffractometer equipped with a copper anode and a multichannel PIXCEL® detector.  
126 Crystalline mineral identification and quantification were obtained for the bulk and fine  
127 soils, as well as generated aerosols (by both the wind tunnel and SyGAVib devices) us-  
128 ing the Highscore Plus 3.0 software and ICSD database (Inorganic Crystal Structure Database).  
129 The MAUD program (Material Analysis Using Diffraction) is a general diffraction pro-  
130 gram mainly based on the Rietveld method (Lutterotti et al., 1999) and is specifically  
131 used for the quantitative phase analysis in this work.

132 The aerosol size distribution was obtained using a MetOne 237B 6 channels (0.3,  
133 0.5, 0.7, 1 and 5  $\mu\text{m}$ ) laser particle counter.

#### 134 **2.4 Statistical compositional analysis**

135 Data processing was performed using the free R software (R Core Team, 2018), specif-  
136 ically with the "compositions" package (K. van den Boogaart et al., 2014) which pro-  
137 vides a set of functions especially designed to process compositional data.

### 138 **3 Results and discussion**

#### 139 **3.1 Structure and crystalline mineralogy**

140 Sand exceeds 91% of the total mass for all soils (Table 1); as a result, the soil sam-  
141 ples are classed as sandy according to the common soil classification (Baize, 2000). Soil  
142 from Ghraïba is the sandiest (98%) and the least silty, whereas that from Kerkennah is  
143 the siltiest, with  $\approx 8\%$  of silt and clay. Different types of aggregates are generally observed  
144 in dry soils from arid and semi-arid regions. These aggregates are either almost exclu-  
145 sively composed of very small individual particles (Alfaro et al., 1997), or of a 'core' (most  
146 often a quartz grain) to which some small clay plates, or assemblages of plates, adhere  
147 (Rajot et al., 2003; Engelbrecht et al., 2009, 2016).

148 Figure 2 shows an example of the four diffractograms obtained for the Ghraïba soils  
149 and derived child samples. A strong decrease in the relative intensity of the quartz diffrac-  
150 tion peaks is observed from bulk soil to generated aerosols, with a simultaneous increase  
151 in the peaks for clay and calcite, which are the major mineral crystalline phases. This  
152 quartz depletion from soil to dust was already observed by Caquineau (2002) on trans-  
153 ported airborne Saharan dust samples collected at Cape Verde, Barbados and Miami,  
154 and also by Engelbrecht et al. (2009) for resuspended aerosols from the middle east. Siev-  
155 ing the bulk soil also decreases the relative quartz content, but to a lesser extent. Re-  
156 gardless of which device was used (SyGAVib or wind tunnel), the diffractograms for the  
157 generated aerosol samples are similar in terms of their pattern as well as their semi-quantitative  
158 results (Figure 3), indicating a comparable mineralogical composition.

#### 159 **3.2 Aerosol size distribution**

160 The size distribution, expressed as the number of particles, of the material produced  
161 by the SyGAVib device is consistent all throughout the experiments; this is apparently  
162 not the case with the wind tunnel experiments as the first replicate is notably enriched  
163 in the finest particles (0.3–0.5  $\mu\text{m}$  channel in Figure 4). Given that this finest fraction  
164 only accounts for less than 1% of the total aerosol mass, this should have little influence  
165 on the overall composition of the collected aerosol, at least on the major and minor el-

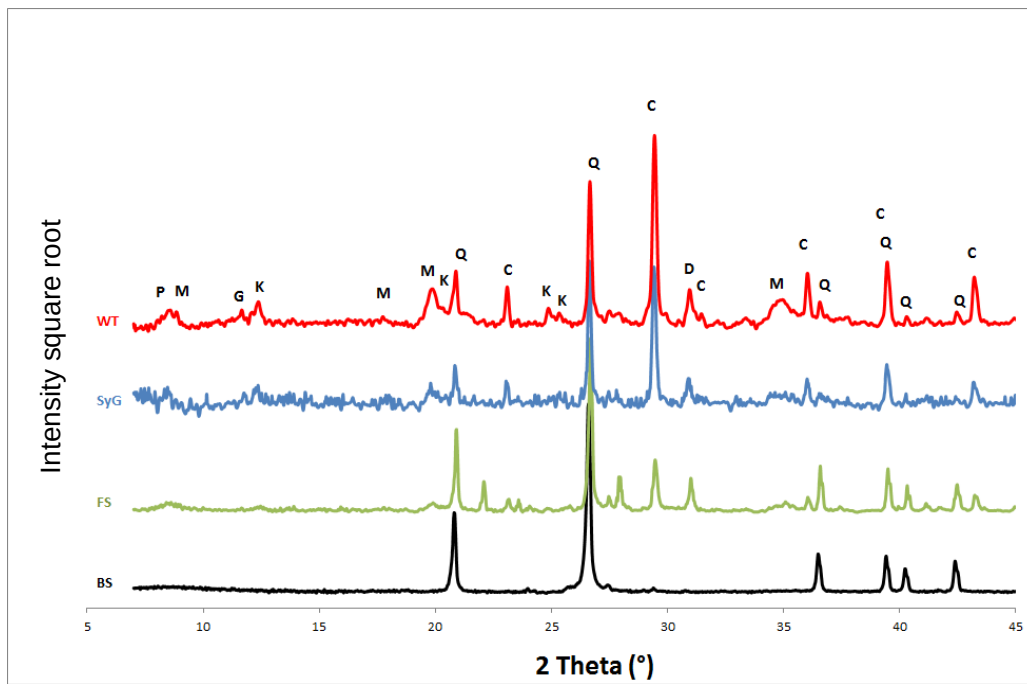


**Figure 2.** Diffractograms of the aerosols generated by the SyGAVib system and the wind tunnel from the Ghraiba soil. Each diffractogram intensity was rescaled to obtain the same average height on a square root scale. Q: quartz, D: dolomite, C: calcite, M: muscovite, K: kaolinite, P: palygorskite, G: gypsum. The diffractograms and semi-quantitative mineralogical composition of the other soils are provided in the supporting information (Figure S1 and Table S2).

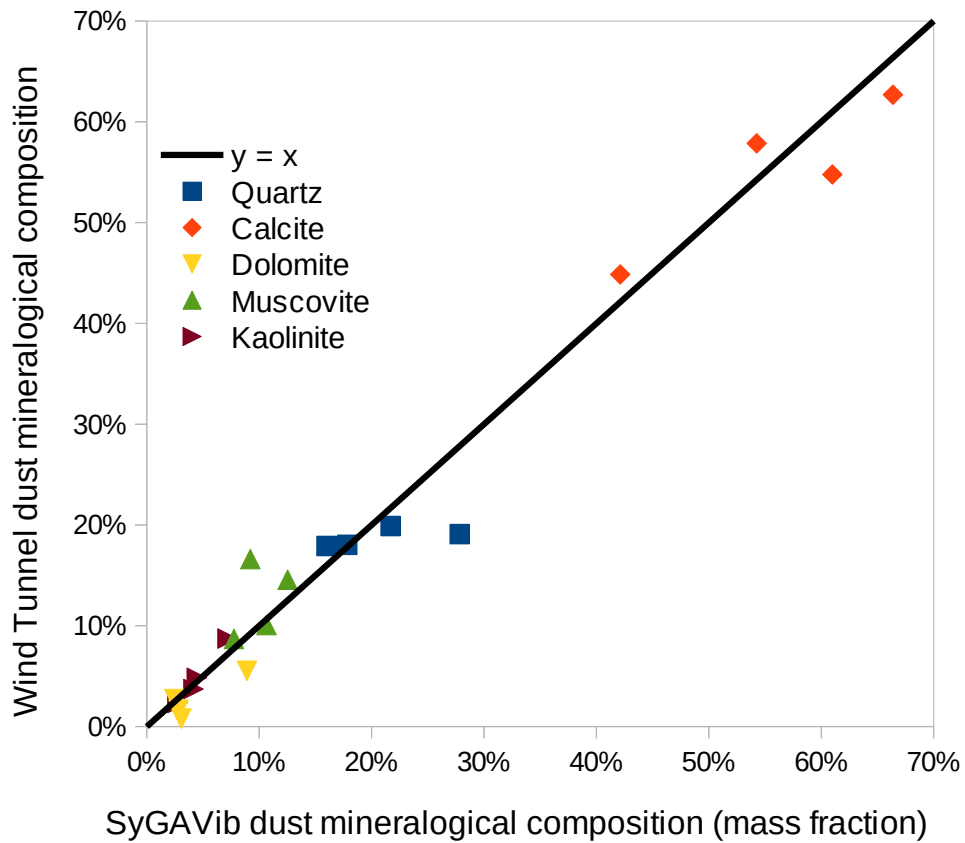


**Figure 3.** Comparison of the semi-quantitative analyses of the major minerals in wind tunnel experiments (WT, y axis) versus Sygavib experiments (Syg, x axis) for the four parent soils aerosol samples. The line  $y = x$  have been drawn.

**Table 2.** Chemical composition of soils and aerosols expressed as oxides. The abbreviations Syg, WT, FS and BS stand for SyGAVib, wind tunnel, Fine Soil and Bulk Soil, respectively. The Syg and WT aerosol samples correspond to the average of the replicates.

	CaO	SiO <sub>2</sub>	Al <sub>2</sub> O <sub>3</sub>	Fe <sub>2</sub> O <sub>3</sub>	MgO	K <sub>2</sub> O	Na <sub>2</sub> O	TiO <sub>2</sub>	SrO	MnO	SO <sub>3</sub>
Attaya_BS	13%	78%	2.7%	1.4%	1.2%	1.1%	0.7%	0.29%	0.08%	0.014%	0.35%
Attaya_FS	28%	45%	9.3%	5.0%	3.7%	2.3%	1.5%	0.90%	0.14%	0.052%	2.1%
Attaya_Syg	34%	32%	8.8%	5.1%	3.7%	2.9%	2.0%	0.68%	0.19%	0.063%	7.5%
Attaya_WT	36%	29%	8.1%	5.7%	3.2%	2.9%	1.9%	0.73%	0.20%	0.070%	7.9%
Cherrarda_BS	3.0%	89%	4.0%	1.4%	0.7%	1.1%	0.06%	0.24%	0.009%	0.009%	0.04%
Cherrarda_FS	18%	59%	11%	5.1%	2.3%	2.3%	0.22%	0.96%	0.045%	0.048%	0.18%
Cherrarda_Syg	31%	43%	13%	6.0%	2.7%	2.5%	0.18%	0.83%	0.050%	0.072%	0.35%
Cherrarda_WT	33%	39%	12%	7.6%	3.0%	3.0%	0.16%	0.96%	0.068%	0.091%	0.48%
Ghraiba_BS	0.7%	96%	1.9%	0.4%	0.41%	0.5%	0.05%	0.11%	0.004%	0.0039%	0.15%
Ghraiba_FS	18%	60%	8.8%	4.5%	3.0%	2.2%	0.39%	1.15%	0.053%	0.045%	0.71%
Ghraiba_Syg	22%	49%	14%	5.1%	3.4%	2.7%	0.36%	0.91%	0.063%	0.079%	1.7%
Ghraiba_WT	18%	47%	15%	6.1%	4.3%	2.9%	0.37%	0.91%	0.061%	0.091%	3.1%
Hsar_BS	9.5%	84%	2.9%	1.5%	0.84%	0.7%	0.07%	0.19%	0.037%	0.008%	<0.1%
Hsar_FS	31%	49%	8.9%	4.6%	3.0%	2.0%	0.25%	0.89%	0.079%	0.035%	0.29%
Hsar_Syg	42%	36%	9.9%	4.2%	3.6%	2.2%	0.23%	0.58%	0.11%	0.053%	0.67%
Hsar_WT	46%	31%	8.4%	6.0%	3.0%	2.7%	0.28%	0.75%	0.14%	0.071%	0.76%

166 elements or phases. Both aerosol generation methods present a maximum number of par-  
 167 ticles within the 2–5  $\mu\text{m}$  fraction, but particles tend to be larger when they are produced  
 168 by the wind tunnel compared with SyGAVib (Figure 4).

### 169 3.3 Chemical composition

170 The elemental compositions expressed as oxides: SiO<sub>2</sub>, Al<sub>2</sub>O<sub>3</sub>, Fe<sub>2</sub>O<sub>3</sub>, CaO, MgO,  
 171 K<sub>2</sub>O, Na<sub>2</sub>O, TiO<sub>2</sub>, SrO, MnO and SO<sub>3</sub>, were measured and averaged for all sample types  
 172 (Table 2, and the measurement dispersion is reported in Table S3 in the supporting in-  
 173 formation).

174 The elemental ratios of the generated aerosols and fine soils over their correspond-  
 175 ing bulk soils were calculated for each soil sample (see Figure 5 for the Cherrarda sam-  
 176 ples, and Figure S2 in the supporting information for the other soils). SiO<sub>2</sub> appears to  
 177 be systematically depleted in all treatments that include sieving and generated aerosols,  
 178 while all the other elements are enriched (their ratios are much higher than one), as al-  
 179 ready pointed out in previous studies (Acosta et al., 2009; Schütz & Rahn, 1982). This  
 180 is particularly obvious in the Ghraiba samples, which exhibited the highest silica con-  
 181 tent. This behaviour can easily be explained by a more or less pronounced diluting ef-  
 182 fect of SiO<sub>2</sub>.

183 This is fully coherent with the larger amount of quartz crystals already identified  
 184 via XRD analysis in bulk soils, and with the mineralogical changes observed after aerosol  
 185 generation. As additional proof, when the elemental composition ratios were calculated  
 186 without SiO<sub>2</sub> (considering the sum of all remaining elements as being equal to 100%),  
 187 all elemental composition ratios tended toward unity (Figure 6). Although the influence  
 188 of SiO<sub>2</sub> is clear enough to be interpreted in a straightforward manner, it is more diffi-  
 189 cult to evaluate the extent to which the elemental composition has been modified by siev-  
 190 ing or by aerosol generation, and to compare the results obtained between them after  
 191 treatment.

192 It is possible to explore the structuration inside a compositional dataset using a  
 193 compositional biplot. This representation expresses the relative variation of a multivari-  
 194 ate dataset by projection onto a plane (J. Aitchison & Greenacre, 2002). Similarly to  
 195 the classic biplot of Gabriel (1971), it allows samples and variables to be depicted to-  
 196 gether. It is worth mentioning, however, that centred log-ratio (clr) transformed data

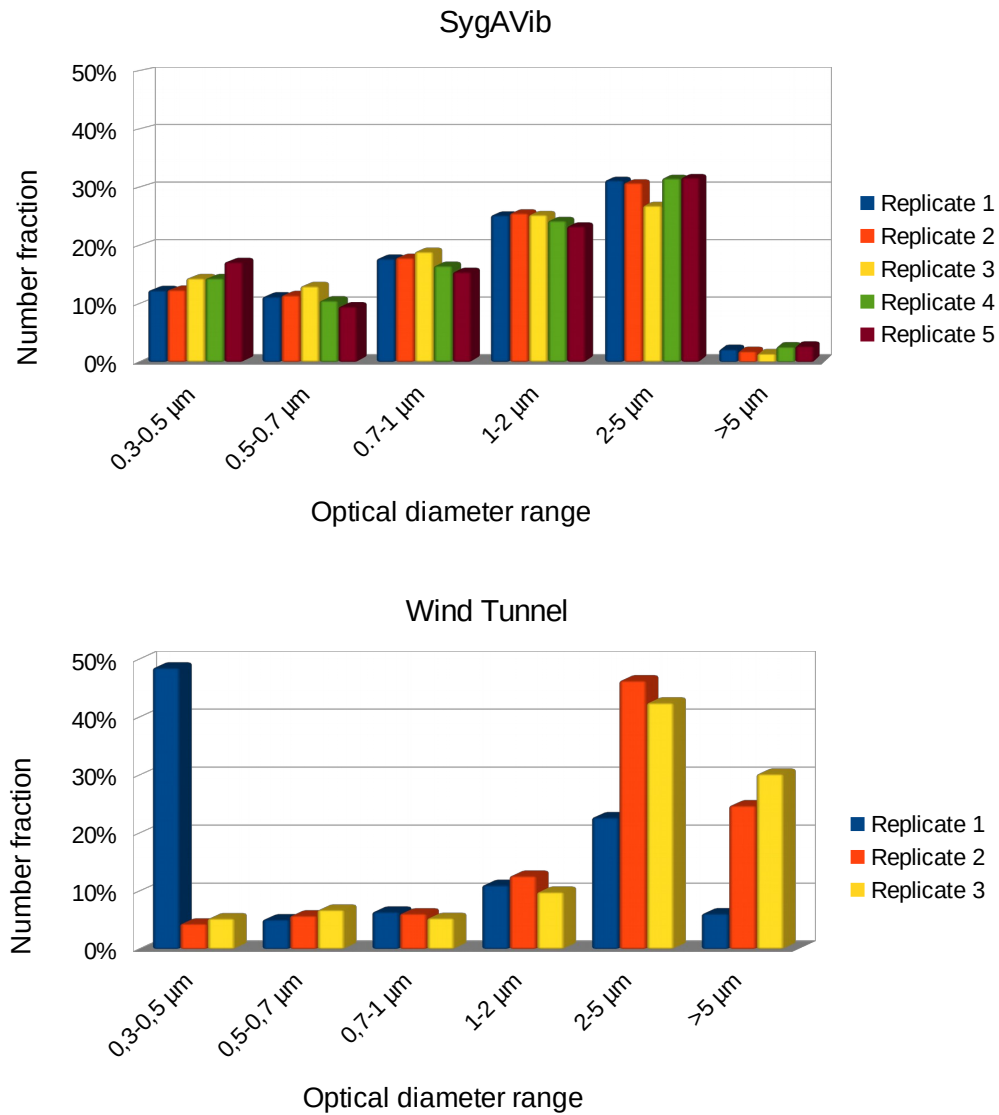


**Figure 4.** Size distributions (in terms of particles number) of the replicates of the dust generated by the SyGAVib system (n=5, 40 min each) and wind tunnel (n=3, 3 min each) averaged for the total duration of each replicate for the Cherarda soil SyGAVib, and WT experiments).

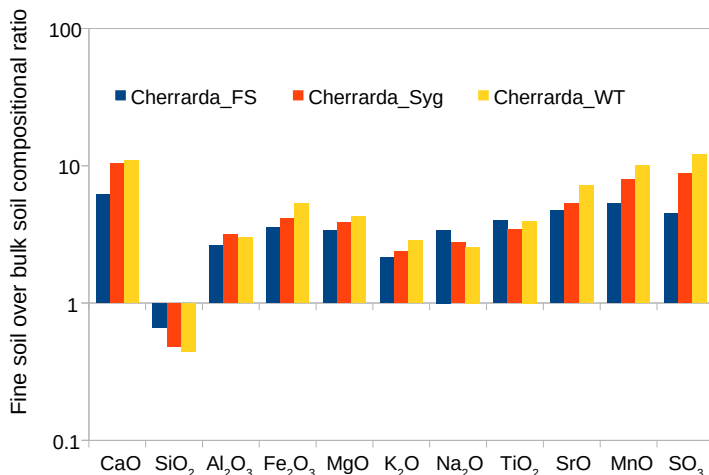


**Figure 5.** Compositional ratios of the generated aerosols and fine soil fraction over the bulk soil, with a logarithmic scale.

197 are used as inputs instead of raw concentrations. The rays formed by variables cannot  
 198 be interpreted directly. Only links between two arrow heads (i.e., the projection of the  
 199 variables) are meaningful, and approximate the standard deviations of the log-ratios of  
 200 these variables. The angle cosines between the links estimate the correlations between  
 201 two log-ratios (for more details see J. Aitchison & Greenacre 2002; K. G. van den Boogaart  
 202 & Tolosana-Delgado 2013). A compositional biplot can therefore be used to examine el-  
 203 elementary ratios (actually pairwise log-ratios) in the individuals, and not their level of  
 204 concentrations, as observed in Gabriel’s biplot. Consequently, the absolute concentra-  
 205 tion values disappear during this statistical analysis which means that all the elemen-  
 206 tal ratios remain instead. A conventional biplot representation cannot be used here be-  
 207 cause spurious correlations due to the interdependence of the components are expected  
 208 in any compositional dataset (Chayes, 1960).

209 The compositional biplot clearly displays the distance between two samples which  
 210 is used as a reliable proxy of compositional similarity in terms of the elemental log-ratios  
 211 (for further more details and the additional properties of the compositional biplots, see  
 212 J. Aitchison & Greenacre (2002); J. M. Aitchison (2005); K. G. van den Boogaart & Tolosana-  
 213 Delgado (2013)). Given that values of zero or those below the detection limit cannot be  
 214 handled in a compositional biplot, SO<sub>3</sub> which is too low to be measured in Hsar BS, is  
 215 removed from the compositional data set. This is not an issue for compositional anal-  
 216 yses because compositional biplots are also suitable for all sub-compositions (J. M. Aitchi-  
 217 son, 2005).

218 Figure 7 is a biplot presenting the results of the compositional data analyses on all  
 219 parent and child samples with a very large dispersion of the log-ratios; in the diagram,  
 220 it can be observed that BS, FS, Syg and WT are well spread out along the SiO<sub>2</sub> axis (de-  
 221 marcatd by a red arrow). The second main split involves log-ratios including sodium.  
 222 It discriminates between the origins of the sample parent soils, but not the nature of the  
 223 sample (BS, FS, WT or Syg). This type of graph presents clearer and more concise com-  
 224 positional variations than the bar graphs shown in Figures 5 and 6, where the dilution  
 225 effect of silica can be seen but not the role of sodium. As mentioned above, the phys-  
 226 ical distance between two points is equivalent to a compositional distance. By remov-  
 227 ing the influence of silica dilution and sodium soil discrimination, the bulk soil chemi-  
 228 cal composition remains clearly different from that of fine sieved soils, or generated aerosols,

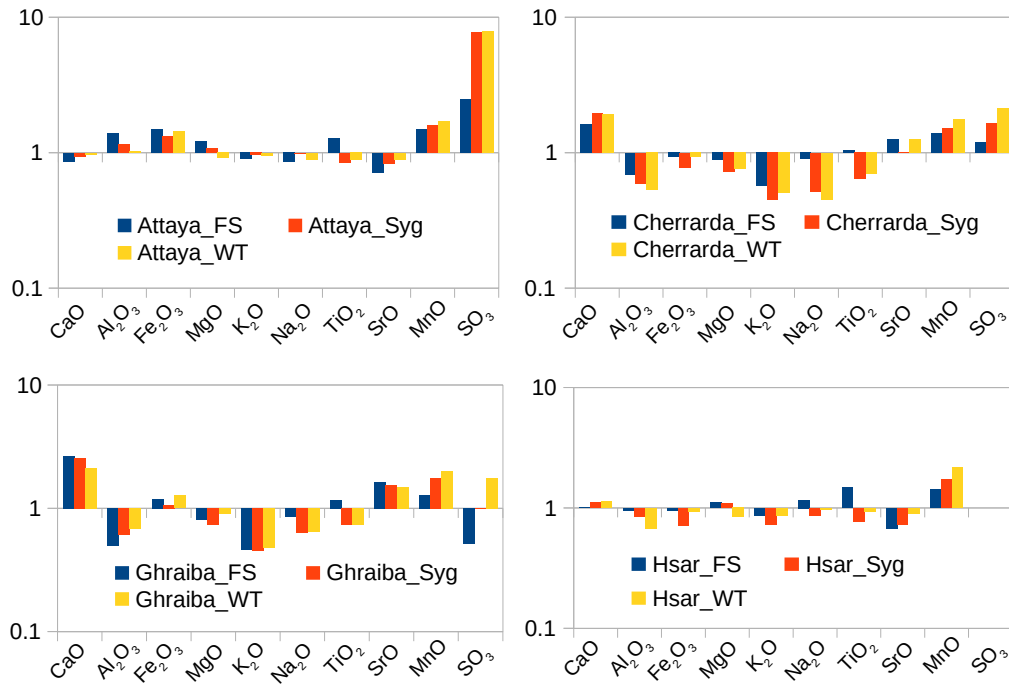


**Figure 6.** Compositional ratios of aerosol and fine soil over bulk soil excluding the silica contribution with a logarithmic scale.

229 with no clear specific contribution of one given element (Figure 8). For each parent soil,  
 230 the SyGAVib, wind tunnel and fine soil generation methods are found relatively close  
 231 together on the biplot diagram and thereby show similar compositions. However there  
 232 were slightly more similarities between the two generated aerosols. The cut-off diame-  
 233 ter, ranging from 56  $\mu\text{m}$  for fine soil to 10  $\mu\text{m}$  for aerosol generations, does not have a  
 234 strong effect on the chemical composition of the resulting material, when calculated with-  
 235 out silica or sodium. Excluding the silica and sodium contribution, the fine sieved soil  
 236 fraction is therefore a good surrogate for generated aerosols for working with internal  
 237 elemental ratios.

### 238 3.4 Comparisons with field sampled aerosols

239 Natural airborne aerosols have been collected and measured on Kerkennah Island,  
 240 close to the bulk soil sampling locations, over a one year period in 2010 and 2011. Sam-  
 241 pling was performed on a mast two meters above the roof of a three levels building in  
 242 a free area using the same filtration system and the same filters (Trabelsi et al., 2016).  
 243 The  $\text{Na}_2\text{O}$ ,  $\text{MgO}$  and  $\text{K}_2\text{O}$  contents of these aerosols were much higher than those of the  
 244 soils and derived aerosols measured in the present study, due to a large contribution of  
 245 sea salt aerosols, especially in winter. To assess the soil contribution to aerosols, these  
 246 three elements were not considered, and samples collected in winter were removed. A  
 247 new compositional biplot including bulk and fine soils, laboratory-generated aerosols, and  
 248 field-sampled aerosols was produced using  $\text{CaO}$ ,  $\text{SiO}_2$ ,  $\text{Al}_2\text{O}_3$  and  $\text{Fe}_2\text{O}_3$  (Figure 9). Field  
 249 sampled aerosols were similar to both SyGAVib and wind tunnel aerosols, and quite dif-  
 250 ferent from bulk soils, due to the variation in the silica content, while fine soils were more  
 251 similar to the aerosol samples than to the parent soils. In this case, aerosols generated

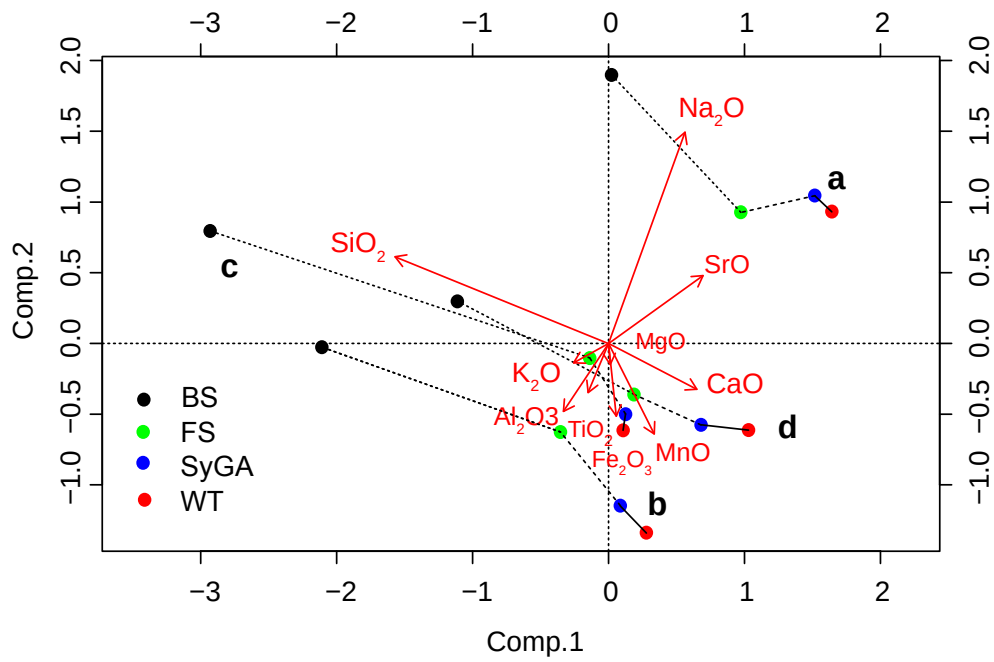


**Figure 7.** Biplot including bulk and fine soils, and generated aerosol. Together Component 1 and Component 2 account for 86% of the total variance (56% and 30%, respectively). **a:** Attaya, **b:** Cherrarda, **c:** Ghraiba, **d:** Hsar. The solid line links the wind tunnel and SyGAVib generated aerosol from the same soil type, the dashed line links the SyGAVib and fine soils of the same soil type.

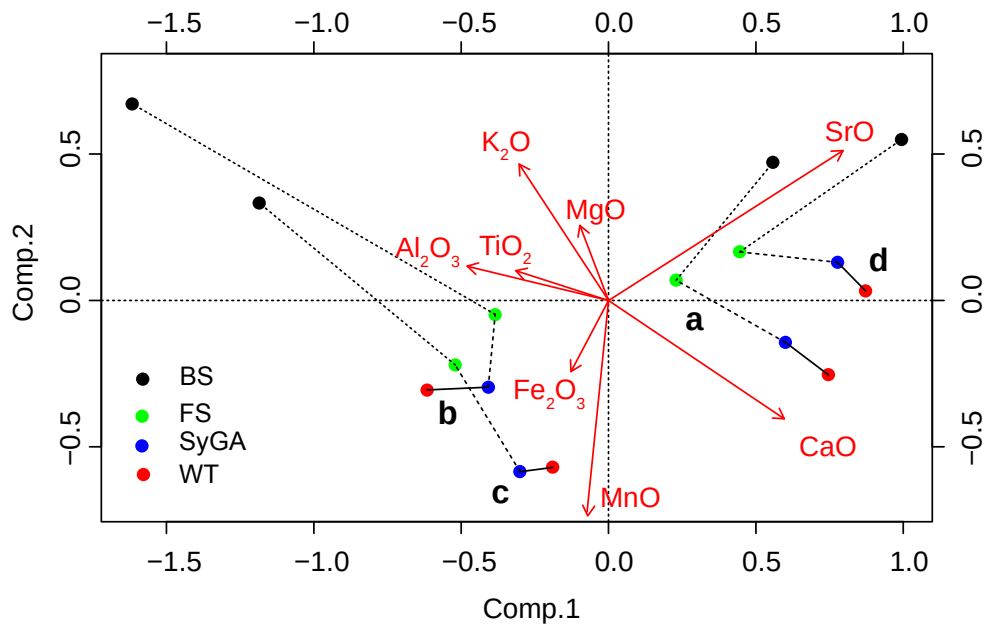


**Figure 8.** Biplot including bulk and fine soils, and generated aerosol excluding the silica and sodium contribution. The solid line links the wind tunnel and SyGAVib generated aerosol from the same soil type, the dashed line links the SyGAVib and fine soils of the same soil type. Together Component 1 and Component 2 account for 86% of the total variance (70% and 16%, respectively). **a:** Attaya, **b:** Cherrarda, **c:** Ghraiba, **d:** Hsar.

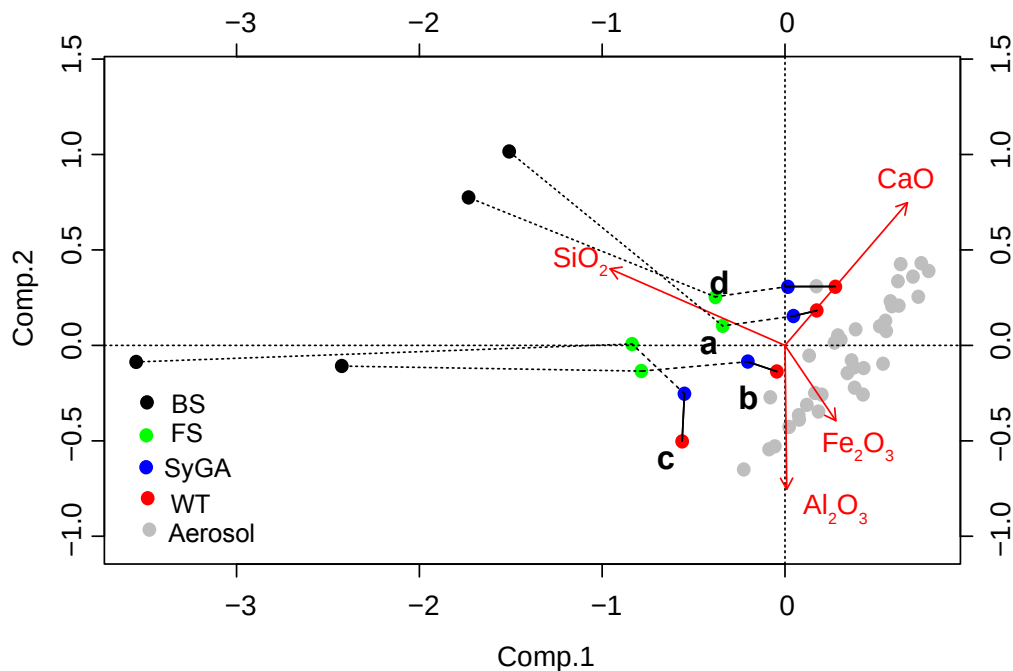


**Figure 9.** Compositional Principal Component Analysis biplot of the soil, laboratory generated aerosols and field aerosols except in winter. Component 1 and Component 2 account for 98% of the variance, with 84% for Component 1. **a:** Attaya, **b:** Cherrarda, **c:** Ghraiba, **d:** Hsar. Lines have the same meaning as in the Figures 7 and 8. Aerosol data are from Trabelsi et al. (2016).

252 by both the SyGAVib and wind tunnel device are approaching close to the airborne crustal  
 253 aerosols collected in the field.

#### 254 4 Conclusions

255 Using the new aerosol generation system by vibration (SyGAVib), it was possible  
 256 to extract a fine soil fraction ( $< 10 \mu\text{m}$ ) with a chemical and mineralogical composi-  
 257 tion similar to wind-generated aerosols for a given soil. This vibration system, which is  
 258 much smaller than a wind tunnel, can be installed on a laboratory bench at a low cost.  
 259 This method does not require large amounts of parent soil ( $\approx 0.5 \text{ g}$ ), it gives a high col-  
 260 lection yield, insures a clean sample without ambient air contamination and it is easy  
 261 to use. Fine sieved soil can also be used as an analogue of aerosol if silica is not to be  
 262 taken into account.

#### 263 Acknowledgments

264 The full data set used to write this paper can be found in supplementary readings and  
 265 also in the AERIS database (<https://doi.org/10.6096/DV/CGVYXC>). We thank Sara  
 266 Mullin correcting the English content and G. Brissebrat for the AERIS database. We  
 267 are grateful to the anonymous reviewers whose judicious comments have improved the  
 268 manuscript.

269 **References**

- 270 Acosta, J., Cano, A. F., Arocena, J., Debela, F., & Martínez-Martínez, S. (2009,  
271 February). Distribution of metals in soil particle size fractions and its implication  
272 to risk assessment of playgrounds in Murcia City (Spain). *Geoderma*, *149*(1-  
273 2), 101–109. Retrieved 2019-10-24, from [https://linkinghub.elsevier.com/  
274 retrieve/pii/S0016706108003431](https://linkinghub.elsevier.com/retrieve/pii/S0016706108003431) doi: 10.1016/j.geoderma.2008.11.034
- 275 Aitchison, J., & Greenacre, M. (2002, October). Biplots of compositional data. *Jour-  
276 nal of the Royal Statistical Society: Series C (Applied Statistics)*, *51*(4), 375–392.  
277 Retrieved 2019-10-24, from <http://doi.wiley.com/10.1111/1467-9876.00275>  
278 doi: 10.1111/1467-9876.00275
- 279 Aitchison, J. M. (2005). A Concise Guide to Compositional Data Analysis.  
280 *Compositional Data Analysis Workshop, CoDaWork'05, Girona Universitat  
281 de Girona*. Retrieved from [http://ima.udg.edu/Activitats/CoDaWork05/  
282 A\\_concise\\_guide\\_to\\_compositional\\_data\\_analysis.pdf](http://ima.udg.edu/Activitats/CoDaWork05/A_concise_guide_to_compositional_data_analysis.pdf)
- 283 Alfaro, S. C. (2008, January). Influence of soil texture on the binding energies of fine  
284 mineral dust particles potentially released by wind erosion. *Geomorphology*, *93*(3-  
285 4), 157–167. Retrieved 2019-10-24, from [https://linkinghub.elsevier.com/  
286 retrieve/pii/S0169555X07000748](https://linkinghub.elsevier.com/retrieve/pii/S0169555X07000748) doi: 10.1016/j.geomorph.2007.02.012
- 287 Alfaro, S. C., Gaudichet, A., Gomes, L., & Maillé, M. (1997, May). Modeling the  
288 size distribution of a soil aerosol produced by sandblasting. *Journal of Geophys-  
289 ical Research: Atmospheres*, *102*(D10), 11239–11249. Retrieved 2019-10-24, from  
290 <http://doi.wiley.com/10.1029/97JD00403> doi: 10.1029/97JD00403
- 291 Alfaro, S. C., & Gomes, L. (1995). Improving the large-scale modeling of the  
292 saltation flux of soil particles in presence of nonerrodible elements. *Jour-  
293 nal of Geophysical Research*, *100*(D8), 16357. Retrieved 2019-10-24, from  
294 <http://doi.wiley.com/10.1029/95JD01281> doi: 10.1029/95JD01281
- 295 Andreae, M. (1995). 10. Climatic Effects of Changing Atmospheric Aerosol Lev-  
296 els. In *Future climates of the world: a modelling perspective* (pp. 341–392). Am-  
297 sterdam; New York: Elsevier. Retrieved from [https://www.elsevier.com/books/  
298 future-climates-of-the-world/henderson-sellers/978-0-444-89322-2](https://www.elsevier.com/books/future-climates-of-the-world/henderson-sellers/978-0-444-89322-2)
- 299 Arimoto, R. (2001, June). Eolian dust and climate: relationships to sources, tropo-  
300 spheric chemistry, transport and deposition. *Earth-Science Reviews*, *54*(1-3), 29–  
301 42. Retrieved 2019-10-24, from [https://linkinghub.elsevier.com/retrieve/  
302 pii/S001282520100040X](https://linkinghub.elsevier.com/retrieve/pii/S001282520100040X) doi: 10.1016/S0012-8252(01)00040-X
- 303 Caquineau, S. (2002). Mineralogy of Saharan dust transported over northwestern  
304 tropical Atlantic Ocean in relation to source regions. *Journal of Geophysical Re-  
305 search*, *107*(D15), 4251. Retrieved 2019-10-24, from [http://doi.wiley.com/10  
306 .1029/2000JD000247](http://doi.wiley.com/10.1029/2000JD000247) doi: 10.1029/2000JD000247
- 307 Chayes, F. (1960, December). On correlation between variables of constant  
308 sum. *Journal of Geophysical Research*, *65*(12), 4185–4193. Retrieved  
309 2019-10-24, from <http://doi.wiley.com/10.1029/JZ065i012p04185> doi:  
310 10.1029/JZ065i012p04185
- 311 Engelbrecht, J. P., McDonald, E. V., Gillies, J. A., Jayanty, R. K. J., Casuccio, G.,  
312 & Gertler, A. W. (2009). Characterizing mineral dusts and other aerosols from  
313 the middle east—part 2: Grab samples and re-suspensions. *Inhalation Toxicology*,  
314 *21*(4), 327–336. Retrieved from <https://doi.org/10.1080/08958370802464299>  
315 doi: 10.1080/08958370802464299
- 316 Engelbrecht, J. P., Moosmüller, H., Pincock, S., Jayanty, R. K. M., Lersch, T.,  
317 & Casuccio, G. (2016). Technical note: Mineralogical, chemical, morpho-  
318 logical, and optical interrelationships of mineral dust re-suspensions. *Atmo-  
319 spheric Chemistry and Physics*, *16*(17), 10809–10830. Retrieved from [https://  
320 www.atmos-chem-phys.net/16/10809/2016/](https://www.atmos-chem-phys.net/16/10809/2016/) doi: 10.5194/acp-16-10809-2016
- 321 Gabriel, K. R. (1971). The biplot graphic display of matrices with application to  
322 principal component analysis. *Biometrika*, *58*(3), 453–467. Retrieved 2019-11-

- 14, from <https://academic.oup.com/biomet/article-lookup/doi/10.1093/biomet/58.3.453> doi: 10.1093/biomet/58.3.453
- Gill, T. E., Zobeck, T. M., & Stout, J. E. (2006, April). Technologies for laboratory generation of dust from geological materials. *Journal of Hazardous Materials*, 132(1), 1–13. Retrieved 2019-10-24, from <https://linkinghub.elsevier.com/retrieve/pii/S0304389405008071> doi: 10.1016/j.jhazmat.2005.11.083
- Gillette, D. (1978, January). Tests with a portable wind tunnel for determining wind erosion threshold velocities. *Atmospheric Environment (1967)*, 12(12), 2309–2313. Retrieved 2019-10-24, from <https://linkinghub.elsevier.com/retrieve/pii/0004698178902718> doi: 10.1016/0004-6981(78)90271-8
- Gomes, L., Bergametti, G., Coudé-Gaussen, G., & Rognon, P. (1990). Submicron desert dusts: A sandblasting process. *Journal of Geophysical Research*, 95(D9), 13927. Retrieved 2019-10-24, from <http://doi.wiley.com/10.1029/JD095iD09p13927> doi: 10.1029/JD095iD09p13927
- Guieu, C., Dulac, F., Ridame, C., & Pondaven, P. (2014, January). Introduction to project DUNE, a DUst experiment in a low Nutrient, low chlorophyll Ecosystem. *Biogeosciences*, 11(2), 425–442. Retrieved 2019-10-24, from <https://www.biogeosciences.net/11/425/2014/> doi: 10.5194/bg-11-425-2014
- Kjelgaard, J. F., Chandler, D. G., & Saxton, K. E. (2004, February). Evidence for direct suspension of loessial soils on the Columbia Plateau. *Earth Surface Processes and Landforms*, 29(2), 221–236. Retrieved 2019-10-24, from <http://doi.wiley.com/10.1002/esp.1028> doi: 10.1002/esp.1028
- Lafon, S., Alfaro, S. C., Chevaillier, S., & Rajot, J. L. (2014, December). A new generator for mineral dust aerosol production from soil samples in the laboratory: GAMEL. *Aeolian Research*, 15, 319–334. Retrieved 2019-10-24, from <https://linkinghub.elsevier.com/retrieve/pii/S1875963714000330> doi: 10.1016/j.aeolia.2014.04.004
- Losno, R., Bergametti, G., & Mouvier, G. (1987, January). Determination of optimal conditions for atmospheric aerosol analysis by X-ray fluorescence. *Environmental Technology Letters*, 8(1-12), 77–86. Retrieved 2019-10-24, from <http://www.tandfonline.com/doi/abs/10.1080/09593338709384465> doi: 10.1080/09593338709384465
- Lutterotti, L., Matthies, S., & Wenk, H. R. (1999). MAUD: a friendly Java program for material analysis using diffraction. In (pp. 1599–1604). Montreal, Canada.
- Mendez, M. J., Panebianco, J. E., & Buschiazzi, D. E. (2013, March). A new dust generator for laboratory dust emission studies. *Aeolian Research*, 8, 59–64. Retrieved 2019-10-24, from <https://linkinghub.elsevier.com/retrieve/pii/S1875963712000651> doi: 10.1016/j.aeolia.2012.10.007
- Monna, F., Marques, A. N., Guillon, R., Losno, R., Couette, S., Navarro, N., ... Nepomuceno, F. (2017, November). Perturbation vectors to evaluate air quality using lichens and bromeliads: a Brazilian case study. *Environmental Monitoring and Assessment*, 189(11), 566. Retrieved 2019-10-24, from <http://link.springer.com/10.1007/s10661-017-6280-0> doi: 10.1007/s10661-017-6280-0
- Pasquet, C., Le Monier, P., Monna, F., Durllet, C., Brigaud, B., Losno, R., ... Gunkel-Grillon, P. (2016, December). Impact of nickel mining in New Caledonia assessed by compositional data analysis of lichens. *SpringerPlus*, 5(1), 2022. Retrieved 2019-10-24, from <http://springerplus.springeropen.com/articles/10.1186/s40064-016-3681-4> doi: 10.1186/s40064-016-3681-4
- R Core Team. (2018). *R: A Language and Environment for Statistical Computing*. Vienna, Austria: R Foundation for Statistical Computing. Retrieved from <http://www.R-project.org/>
- Rajot, J., Alfaro, S., Gomes, L., & Gaudichet, A. (2003, August). Soil crusting on sandy soils and its influence on wind erosion. *CATENA*, 53(1), 1–16. Re-

- 377        retrieved 2019-10-24, from [https://linkinghub.elsevier.com/retrieve/pii/](https://linkinghub.elsevier.com/retrieve/pii/S0341816202002011)  
378        S0341816202002011 doi: 10.1016/S0341-8162(02)00201-1
- 379        Salam, A., Lohmann, U., Crenna, B., Lesins, G., Klages, P., Rogers, D., ... Coffin,  
380        M. (2006, February). Ice Nucleation Studies of Mineral Dust Particles with a  
381        New Continuous Flow Diffusion Chamber. *Aerosol Science and Technology*, 40(2),  
382        134–143. Retrieved 2019-10-24, from [http://www.tandfonline.com/doi/abs/](http://www.tandfonline.com/doi/abs/10.1080/02786820500444853)  
383        10.1080/02786820500444853 doi: 10.1080/02786820500444853
- 384        Schütz, L., & Rahn, K. A. (1982, January). Trace-element concentrations in erodible  
385        soils. *Atmospheric Environment (1967)*, 16(1), 171–176. Retrieved 2019-10-24,  
386        from <https://linkinghub.elsevier.com/retrieve/pii/0004698182903249>  
387        doi: 10.1016/0004-6981(82)90324-9
- 388        Trabelsi, A., Masmoudi, M., Quisefit, J., & Alfaro, S. (2016, March). Compositional  
389        variability of the aerosols collected on Kerkennah Islands (central Tunisia). *Atmo-*  
390        *spheric Research*, 169, 292–300. Retrieved 2019-10-24, from [https://linkinghub](https://linkinghub.elsevier.com/retrieve/pii/S0169809515003397)  
391        [.elsevier.com/retrieve/pii/S0169809515003397](https://linkinghub.elsevier.com/retrieve/pii/S0169809515003397) doi: 10.1016/j.atmosres.2015  
392        .10.018
- 393        van den Boogaart, K., Tolosana-Delgado, R., & Bren, M. (2014). *compositions:*  
394        *Compositional Data Analysis. R package version 1.40-1*. Retrieved from [https://](https://CRAN.R-project.org/package=compositions)  
395        CRAN.R-project.org/package=compositions
- 396        van den Boogaart, K. G., & Tolosana-Delgado, R. (2013). *Analyzing compositional*  
397        *data with R*. Heidelberg: Springer. (OCLC: ocn827083643)